

Anomalous behavior of the first excited 0^+ state in $N \approx Z$ nuclei

K. Kaneko¹, R. F. Casten², M. Hasegawa³, T. Mizusaki⁴,

Jing-ye Zhang^{2,5}, E. A. McCutchan², N. V. Zamfir², R. Krücken⁶

¹Department of Physics, Kyushu Sangyo University, Fukuoka 813-8503, Japan

²WNSL, Yale University, New Haven, Connecticut 06520-8124, USA

³Laboratory of Physics, Fukuoka Dental College, Fukuoka 814-0193, Japan

⁴Institute of Natural Sciences, Senshu University, Kawasaki, Kanagawa, 214-8580, Japan

⁵Department of Physics and Astronomy, University of Tennessee, Knoxville, Tennessee 37996, USA

⁶Physik Department E12, Technische Universität München, 85748 Garching, Germany

(Dated: February 2, 2019)

A study of the energies of the first excited 0^+ states in all even-even $Z \geq 8$ nuclei reveals an anomalous behavior in some nuclei with $N = Z$, $Z \pm 2$. We analyze these irregularities in the framework of the shell model. It is shown that proton-neutron correlations play an important role in this phenomenon.

PACS numbers: 21.10.Re, 21.60.Fw, 27.70.+q

A topic of current interest and varying interpretations is the nature of excited $J^\pi = 0^+$ states in nuclei. Traditionally, the lowest excited 0^+ states in even-even deformed nuclei have been interpreted as “ β ” vibrations[1]. In recent years, various papers [2, 3, 4, 5, 6] have discussed the lowest $K = 0^+$ excitation as a collective excitation built on the γ vibration. The observation of numerous excited 0^+ states in ^{158}Gd [7] prompted several theoretical interpretations. These include their description as two-phonon octupole in character [8] or as quasi-particle excitations based on the projected shell model[9]. In light nuclei, descriptions in terms of pairing vibrations, multi-particle - multi-hole intruder states and isobaric analog states have been discussed for decades. Nevertheless, to date, a complete understanding of the origin of excited 0^+ states remains elusive.

The purpose of this Rapid Communication is twofold. First, we will show a striking, and heretofore unrecognized, anomaly in 0_2^+ energies that occurs in certain (but not all) light nuclei with $N = Z$, $N = Z \pm 2$. Secondly, we will present shell model calculations that show the significant role of the $T = 0$ part of the residual proton-neutron interaction in these anomalies.

With the high current interest in $N \sim Z$ nuclei and the likelihood that new examples of such nuclei will be studied in greater detail with exotic beam experiments in upcoming years, the discovery of new phenomena in such nuclei takes on heightened interest. Looking over the entire nuclear chart, the trend of first excited 0^+ energies exhibits an interesting behavior. To compare nuclei over a wide range of structures, we normalize the energy of the 0_2^+ state by the energy of the 2_1^+ state, defining $R_{0/2} \equiv E(0_2^+)/E(2_1^+)$. This $R_{0/2}$ ratio is plotted as a function of the energy of the first 2_1^+ state in Fig. 1, for all even-even nuclei with $Z \geq 8$. For the majority of nuclei, the $R_{0/2}$ ratios follow a compact trajectory. There are, however, obvious deviations from this trajectory: 7 points which clearly stand out above the main trajectory.

Interestingly, the deviations in Fig. 1 comprise a set of nuclei with $N = Z$ and $N = Z \pm 2$, specifically $^{20,22}\text{Ne}$,

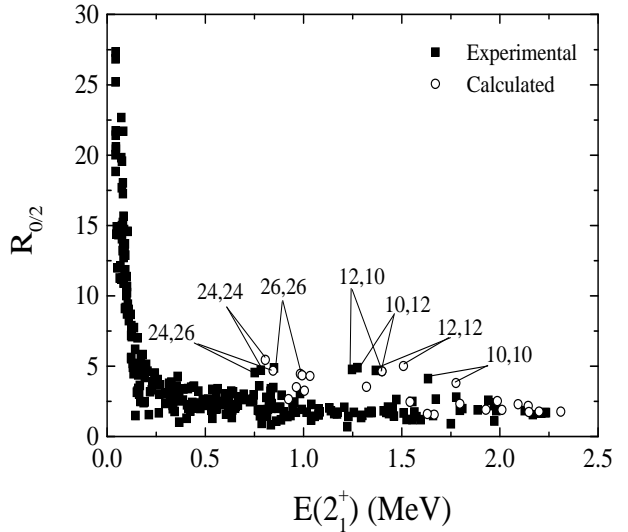


FIG. 1: The energy ratio $R_{0/2} \equiv E(0_2^+)/E(2_1^+)$ as a function of the energy of the first excited 2_1^+ state for all even-even nuclei with $Z \geq 8$. The points above the main trajectory are labelled by their (Z, N) values. The solid squares denote the experimental values and the open circles denote the calculated values for some of these nuclei (see text). The three unlabelled, calculated points that lie above the trajectory near $E(2_1^+) \sim 1.0$ and 1.3 MeV correspond to $^{44,46,48}\text{Ti}$.

$^{22,24}\text{Mg}$, $^{48,50}\text{Cr}$ and ^{52}Fe with Z and/or $N = 10, 12, 24$, and 26. An important aspect of the anomaly is that not all nuclei with $N = Z$, $Z \pm 2$ exhibit it. Specifically, nuclei with N or Z magic or with N or $Z = 14, 16, 18$ or 22 lie within the main trajectory. The phenomenon occurs when, in the most simple view of shell filling, there is an open $1d_{5/2}$ shell or an open $1f_{7/2}$ shell, except for $N, Z = 22$. Any interpretation of this phenomenon must account not only for its existence, but also its locus and must explain why it is not universal in $N = Z$ and $N = Z \pm 2$ light nuclei.

Inspection of the individual excitation energies $E(0_2^+)$

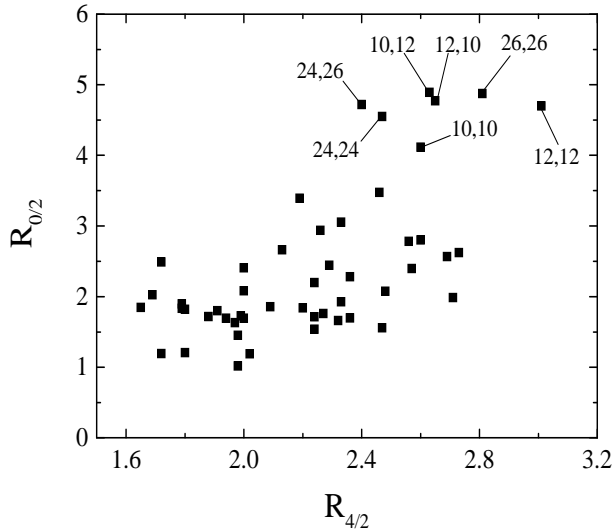


FIG. 2: The energy ratio $R_{0/2}$ as a function of $R_{4/2}$ for *sd* and *fp* shell even-even nuclei with $8 \leq Z \leq 30$. Those nuclei with anomalous $R_{0/2}$ values are labelled by their (Z, N) values.

and $E(2_1^+)$ shows that the ratio $R_{0/2}$ is large for these nuclei due to the combination of a large value of $E(0_2^+)$ and a small value of $E(2_1^+)$ compared with neighbors in the corresponding mass region. Since small 2_1^+ excitation energies are in general associated with soft or deformed nuclei, we investigate the connection between $R_{0/2}$ and deformation in Fig. 2, focusing on the region, $8 \geq Z \geq 30$, where the anomalies are located. As a measure of the structure, we use the energy ratio $R_{4/2} = E(4_1^+)/E(2_1^+)$, where $R_{4/2} = 2.0$ for spherical nuclei, 3.33 for axially deformed nuclei. As the low 2_1^+ energy suggests, each of the anomalous nuclei have $R_{4/2} > 2.4$. However, from Fig. 2, one can also see that there are several other nuclei which have similar structure but do not exhibit an anomalous $R_{0/2}$. This observation reiterates that the anomaly results from a combination of a low 2_1^+ excitation energy and a high 0_2^+ excitation energy.

The remainder of this paper will focus on the origin of the high lying 0_2^+ states in these nuclei using shell model calculations. Since the abnormalities in $R_{0/2}$ occur for nuclei with $N \approx Z$, an appropriate aspect to consider is $p-n$ interactions, which are strong for $N = Z$ nuclei and play a significant role in determining their structure [10]. Numerous studies of $p-n$ correlations incorporating the competition between $T = 0$ and $T = 1$ components have investigated the energy spectrum as well as the binding energy of proton rich nuclei. The large $p-n$ correlations at $N \approx Z$ give rise to several interesting phenomena such as singularities in the $p-n$ interaction energy[11, 12, 13], alpha-like correlations[14], the Wigner energy[15], and degenerate $T = 0$ and $T = 1$ lowest states in odd-odd, $N = Z$ nuclei[16, 17, 18, 19, 20, 21]. We can expect that large $p-n$ correlations may also contribute to the properties of the 0_2^+ state in $N \approx Z$ nuclei.

In order to analyze the above behavior of the 0_2^+

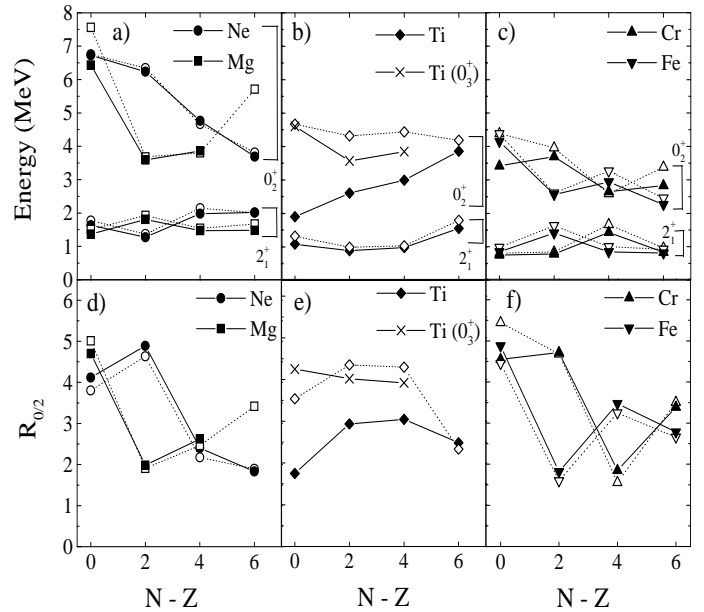


FIG. 3: Excitation energies of the first excited 0^+ and 2^+ states and as a function of $N - Z$ for the (a) Ne and Mg (b) Ti and (c) Cr and Fe isotopes. Ratio $R_{0/2} \equiv E(0_2^+)/E(2_1^+)$ as a function of $N - Z$ for the (d) Ne and Mg (e) Ti and (f) Cr and Fe isotopes. The solid and open symbols denote the experimental and calculated values, respectively. The cross symbols in (b) and (e) correspond to the second excited 0^+ state in the Ti isotopes.

state in $N \approx Z$ nuclei, we perform full shell model calculations for a wide range of nuclei. For the *sd* shell, with model space $(1d_{5/2}, 2s_{1/2}, 1d_{3/2})$, we adopt the Wildenthal interaction[22] to perform calculations for $^{20-26}\text{Ne}$, $^{22-30}\text{Mg}$, $^{28-32}\text{Si}$, $^{32-34}\text{S}$, ^{36}Ar . We note that, in terms of energies, the results obtained for the *sd* shell are identical to those obtained in shell model calculations by Brown[23]. For the *fp* shell, with model space $(1f_{7/2}, 2p_{3/2}, 1f_{5/2}, 2p_{1/2})$, we make use of the KB3 interaction[24] for calculations on $^{44-50}\text{Ti}$, $^{48-54}\text{Cr}$ and $^{52-58}\text{Fe}$. Due to the enormous size of the configuration space for $^{54-58}\text{Fe}$, we employed an extrapolation method[25] for the shell model calculations of these nuclei. The calculated values of $R_{0/2}$ are indicated by the open circles in Fig. 1 and follow very well the experimental trend. In particular, the large deviations from the simple trajectory for the seven nuclei near $N \approx Z$ are well reproduced. The calculations for the remaining nuclei lie within the main trajectory, with the exception of 3 points corresponding to $^{44-48}\text{Ti}$. This peculiarity associated with the Ti nuclei will be discussed below.

A comparison with experimental 0_2^+ and 2_1^+ energies as a function of $N - Z$ for Ne and Mg is given in Fig. 3(a) and for the Cr and Fe isotopes in Fig. 3(c). Included are all seven nuclei previously highlighted, except for ^{22}Mg which should be identical to ^{22}Ne assuming isospin invariance. For $^{20,22}\text{Ne}$ and $^{48,50}\text{Cr}$, i.e., with $N = Z$, $Z + 2$, the 0_2^+ energies are large while the 2_1^+ energies are

small. As neutron number increases, the 0_2^+ energy decreases and the 2_1^+ energy increases. In the Mg and Fe isotopes, the 0_2^+ energy is large only for ^{24}Mg and ^{52}Fe ($N = Z$) and then decreases with neutron excess. The experimental trends of the 0_2^+ and 2_1^+ energies are reproduced well by the calculations. Figures 3(d) and (f) show the corresponding experimental and calculated $R_{0/2}$ ratios. As expected from the discussion of the 0_2^+ and 2_1^+ energies, the ratios for $^{20,22}\text{Ne}$ and $^{48,50}\text{Cr}$ are large and almost two times those of the heavier Ne and Cr isotopes. In the Mg and Fe isotopes, however, the ratios for ^{26}Mg and ^{54}Fe ($N = Z + 2$, with $N = 14$ and $Z = 28$) are small while those of ^{24}Mg and ^{52}Fe ($N = Z$) are large. Again, the experimental behavior is reproduced by the calculations.

While the anomaly for $N = Z$ and $N = Z \pm 2$ nuclei is widespread in the open $1d_{5/2}$ and $1f_{7/2}$ shell nuclei, it is conspicuously absent experimentally in the Ti isotopes. In contrast, in these same nuclei, the 0_2^+ state and $R_{0/2}$ ratio is actually very low in energy as seen in Figs 3(b) and (e). This result is not found in the calculations. They predict the anomaly in $^{44,46}\text{Ti}$ and even in ^{48}Ti ($N = Z + 4$). A recent new effective interaction, GXPF1[26], yields similar results for the Ti isotopes. The explanation of this lies in the well-known presence of low lying 0^+ intruder states in Ti arising from $2p$ - $2h$ proton and $2p$ - $2h$ neutron excitations across the $Z, N = 20$ shell gap, which leads to a collective, low-lying 0_2^+ state. This state is clearly beyond the space of the present calculations. The reason that such a mode is not found in Fe, for example, is simply that the excitation of 2 protons from below $Z = 20$ in Fe ($Z = 26$) would lead to a filled $f_{7/2}$ proton shell with the consequent decrease, rather than increase, in the number of valence protons. Indeed, in other nuclei with a filled $1f_{7/2}$ shell, (i.e., ^{54}Fe) the anomaly is also not found. The 0_3^+ states in the Ti isotopes (crosses in Fig. 3) likely correspond to an fp shell excitation and their energies are reproduced reasonably well by the calculations (open diamonds).

While we have shown that shell model calculations can reproduce the anomalous behavior of $R_{0/2}$, a more detailed analysis of the calculations is required to understand how and why such good agreement is obtained. We first consider the following Hamiltonian:

$$H = H_{sp} + V_{int}, \quad (1)$$

where H_{sp} is the single particle Hamiltonian and V_{int} is the realistic shell model interaction, such as the Wildenthal interaction as used in the following analysis. To examine the roles of the $T = 0$ and $T = 1$ correlations in the 0_2^+ state, we separate the shell model interaction V_{int} into two parts corresponding to the isoscalar, $V_{T=0}$, and isovector, $V_{T=1}$, interactions as follows:

$$V_{int} = V_{T=0} + V_{T=1} \quad (2)$$

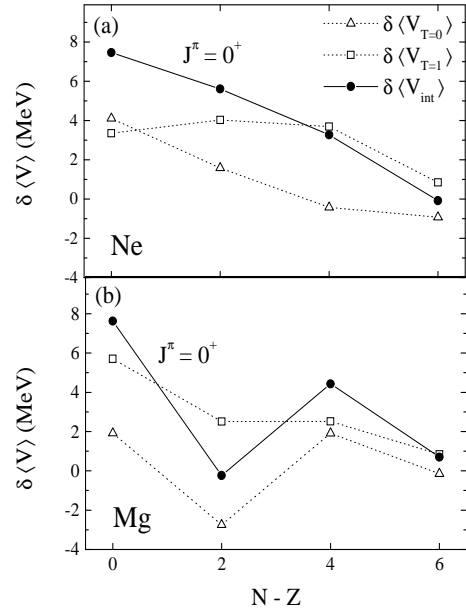


FIG. 4: Correlation energy differences, $\langle V_{int} \rangle$ and the corresponding $T = 0$ and $T = 1$ components for the (a) Ne and (b) Mg isotopes.

To examine the contributions of the $T = 0$ and $T = 1$ components in the shell model interaction, we can calculate their expectation values in the eigenstates of the full Hamiltonian, Eq. (1). Since the excitation energy depends strongly upon the competition between the correlation energies of the excited state and the ground state, we define the following correlation energy difference:

$$\delta\langle O \rangle = \langle O \rangle_{ex} - \langle O \rangle_{gr}, \quad (3)$$

where $\langle O \rangle_{gr}$ and $\langle O \rangle_{ex}$ denote the expectation values of the operator O for the ground and first excited 0^+ states, respectively, and O is a physical operator such as the shell model interaction, V_{int} or the $T = 0, 1$ interactions.

Figure 4 shows the correlation energy difference of 0^+ states as a function of $N - Z$ in the Ne and Mg isotopes, including the shell model interaction energy, $\langle V_{int} \rangle$, and its decomposition into isoscalar, $\langle V_{T=0} \rangle$, and isovector, $\langle V_{T=1} \rangle$, parts. From Fig. 4 we see a correspondence between the ratio $R_{0/2}$ in Fig. 3(d) and the correlation energy differences, $\delta\langle V_{int} \rangle$. For each of the Ne and Mg nuclei, with the exception of ^{20}Ne , the $T = 1$ component is larger than the $T = 0$ component. In the Mg isotopes, Fig. 4(b), the overall evolution of the correlation energy difference, $\delta\langle V_{int} \rangle$, follows very closely the behavior of the $T = 0$ component. Both the $R_{0/2}$ value and correlation energy difference are large in ^{24}Mg and decrease suddenly in ^{26}Mg . This is attributed to the $T = 0$ component, which displays a singular negative value for $N - Z = 2$, resulting in a sudden decrease in $\delta\langle V_{int} \rangle$. For the Ne isotopes, shown in Fig. 4(a), the $T = 1$ component remains relatively constant (~ 3.5 MeV) for $N = 10$

- 14 dropping to ~ 1 MeV for $N = 16$. Because of the nearly constant behavior of the $T = 1$ component, the correlation energy differences in the Ne isotopes follow the trend of the $T = 0$ component, decreasing smoothly with increasing neutron number. This behavior results in large correlation energy differences in the Ne isotopes with $N = Z$ and $N = Z + 2$, which will generate high excitation energies for the 0_2^+ state in these nuclei compared to isotopes with larger N . Thus, the behavior of correlation energy differences, which strongly affects the ratio $R_{0/2}$, is attributed to the combined effects of $T=1$ and $T=0$ components. The former contributes the main amplitude, while the latter correlates with variations in $R_{0/2}$.

From the above discussion, we might expect large values of the ratio $R_{0/2}$ for all nuclei with $N = Z$. However, as previously mentioned, not all nuclei with $N = Z$, $Z \pm 2$ are anomalous. The phenomenon occurs when there is an open $1d_{5/2}$ shell or an open $1f_{7/2}$ shell, except for $N, Z = 22$. We now focus on the $N = Z$ sd -shell nuclei and address why only ^{20}Ne and ^{24}Mg exhibit large $R_{0/2}$ ratios. Figure 5(a) illustrates the excitation energies of the 0_2^+ and 2_1^+ states and the corresponding $R_{0/2}$ ratios. Again, the excitation energies are well reproduced by the shell model calculations. Compared with neighboring $N = Z$ nuclei, ^{20}Ne and ^{24}Mg exhibit large excitation energies of the 0_2^+ states, small excitation energies of the 2_1^+ states and therefore large $R_{0/2}$ ratios. The correlation energy differences, along with their $T = 0$ and $T = 1$ components, are given in Fig. 5(b). The former are

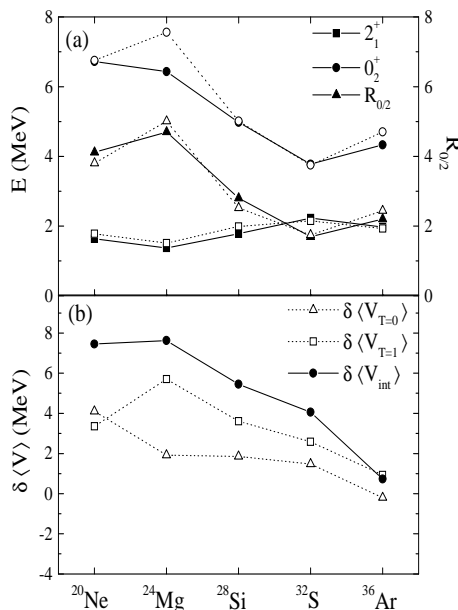


FIG. 5: (a) Excitation energies of the 0_2^+ and 2_1^+ states and the corresponding $R_{0/2}$ ratios for the $N = Z$ sd -shell nuclei. The solid and open symbols denote the experimental and calculated values, respectively. (b) Correlation energy differences $\langle V_{int} \rangle$ and the corresponding $T = 0$ and $T = 1$ components for the $N = Z$ sd -shell nuclei.

large for ^{20}Ne and ^{24}Mg and decrease smoothly with increasing proton number. The behavior of the 0_2^+ states in Fig. 5(a) is similar to that of the correlation energy differences, $\delta \langle V_{int} \rangle$, in Fig. 5(b), with the exception of ^{36}Ar . A similar behavior as described above is observed in the $N = Z + 2$ nuclei. For these nuclei, only ^{22}Ne displays a large $R_{0/2}$ ratio and with increasing proton number, the ratio decreases rapidly.

In conclusion, we have investigated the first excited 0^+ states in light even-even nuclei. It is found that an anomaly occurs in the ratio $R_{0/2} \equiv E(0_2^+)/E(2_1^+)$ in some even-even $N \approx Z$ nuclei. The anomaly results from the combination of large $E(0_2^+)$ energies and small $E(2_1^+)$ energies. The latter are associated with a softness to deformation in these nuclei. Shell model calculations reproduce well the observed behavior. Concentrating on the Ne and Mg isotopes, the anomalies of the 0_2^+ states were analyzed using the correlation energy differences and a decomposition of the shell model interaction into $T = 0$ and $T = 1$ components. From this analysis, it is shown that the anomalous $R_{0/2}$ values can be attributed to the joint effects of the $T = 0$ and $T = 1$ components: the $T=1$ component contributes to the main amplitude while the $T=0$ component correlates with the variation of $R_{0/2}$.

We are grateful to B. A. Brown, R. Broglia, Larry Zamick and Igal Talmi for inspiring discussions. This work was supported by U.S. DOE Grant Nos. DE-FG02-91ER-40609 and DE-FG05-96ER-40983.

[1] A. Bohr and B.R. Mottelson, *Nuclear Structure* (Benjamin, New York, 1975).

[2] R.F. Casten and P. von Brentano, Phys. Rev. C **50**, R1280 (1994).

[3] D.G. Burke and P.C. Sood, Phys. Rev. C **51**, 3525 (1995).

[4] K. Kumar, Phys. Rev. C **51**, 3524 (1995).

[5] C. Günther, S. Boehmsdorff, K. Freitag, J. Manns, and U. Müller, Phys. Rev. C **54**, 679 (1996).

[6] P.F. Garrett, J. Phys. G **27**, R1 (2001).

[7] S.R. Lesher, A. Aprahamian, L. Trache, A. Oros-Peusquens, S. Deyliz, A. Gollwitzer, R. Hertenberger, B.D. Valnion, and G. Graw, Phys. Rev. C **66**, 051305(R) (2002).

[8] N.V. Zamfir, Jing-ye Zhang, and R.F. Casten, Phys. Rev. C **66**, 057303 (2002).

[9] Y. Sun, A. Aprahamian, Jing-ye Zhang, and C.-T. Lee, Phys. Rev. C **68**, 061301(R) (2003).

[10] A.L. Goodman, Adv. Nucl. Phys. **11**, 263 (1979).

[11] Jing-ye Zhang, R.F. Casten, and D.S. Brenner, Phys. Lett. B **227**, 1 (1989).

[12] N. V. Zamfir and R. F. Casten, Phys. Rev. C **43**, 2879 (1991).

[13] K. Kaneko and M. Hasegawa, Phys. Rev. C **60**, 024301 (1999).

[14] M. Hasegawa and K. Kaneko, Phys. Rev. C **61**, 037306 (2000).

[15] W. Satula, D. J. Dean, J. Gary, S. Mizutori, and W. Nazarewicz, Phys. Lett. B **407**, 103 (1997).

[16] N. Zeldes and S. Liran, Phys. Lett. B **62**, 12 (1976).

[17] P. von Brentano, A.F. Lisetskiy, I. Schneider, C. Friebner, R.V. Jolos, N. Pietralla, and A. Schmidt, Prog. Part. Nucl. Phys. **44** 29, (2000).

[18] P. Vogel, Nucl. Phys. A **662**, 148 (2000).

[19] A. O. Macchiavelli *et al.*, Phys. Rev. C **61** 041303(R) (2000); Phys. Lett. B **480**, 1 (2000).

[20] W. Satula and R. Wyss, Phys. Rev. Lett. **86**, 4488 (2001); **87**, 052504 (2001).

[21] K. Kaneko and M. Hasegawa, Phys. Rev. C. **69**, 061302(R) (2004).

[22] B.A. Brown and B.H. Wildenthal, Ann. Rev. Nucl. Phys. Part. Sci. **38**, 29 (1988).

[23] <http://www.nscl.msu.edu/~brown/sde.htm>

[24] A. Poves and A. P. Zuker, Phys. Rev. **70**, 235 (1981); E. Caurier, A. P. Zuker, A. Poves, and G. Martinez-Pinedo, Phys. Rev. C **50**, 225 (1994).

[25] T. Mizusaki and M. Imada, Phys. Rev. C **65**, 064319 (2002); C **67**, 041301(R) (2003).

[26] M. Honma, T. Otsuka, B.A. Brown, and T. Mizusaki, Phys. Rev. C **69**, 034335 (2004).